ResearchGate

See discussions, stats, and author profiles for this publication at: https://www.researchgate.net/publication/280086880

Unambiguous Evidence for a Highly Mobile Surface Layer in Ultrathin Polymer Films by Specific Heat Spectroscopy on Blends

ARTICLE *in* MACROMOLECULES · JULY 2015

Impact Factor: 5.8 · DOI: 10.1021/acs.macromol.5b01259

CITATION
1

READS
29

3 AUTHORS:

Huajie Yin
Bundesanstalt für Materialforschung und -prü…
14 PUBLICATIONS **200** CITATIONS
SEE PROFILE

Sherif Madkour
Bundesanstalt für Materialforschung und -prü…
5 PUBLICATIONS **3** CITATIONS
SEE PROFILE

A. Schönhals
Bundesanstalt für Materialforschung und -prü…
187 PUBLICATIONS **3,643** CITATIONS
SEE PROFILE

Available from: Sherif Madkour
Retrieved on: 27 January 2016

Macromolecules

Article

pubs.acs.org/Macromolecules

Unambiguous Evidence for a Highly Mobile Surface Layer in Ultrathin Polymer Films by Specific Heat Spectroscopy on Blends

Huajie Yin, Sherif Madkour, and Andreas Schönhals*

BAM Bundesanstalt für Materialforschung und -prüfung, Unter den Eichen 87, 12205 Berlin, Germany

ABSTRACT: Despite the decade long controversial discussion on the effect of nanometer confinement on the glass transition temperature (T_g) of ultrathin polymer films, there is still no consistent picture. Here, the dynamic calorimetric glass transition of ultrathin films of a blend, which is miscible in the bulk, is directly investigated by specific heat spectroscopy. By a self-assembling process, a nanometer thick surface layer with a higher molecular mobility is formed at the polymer/air interface. By measuring the dynamic calorimetric T_g in dependence on the film thickness, it was shown that the T_g of the whole film was strongly influenced by that nanometer thick surface layer, with a lower T_g. Since the observed thickness dependence of the dynamic T_g is similar to the thickness dependence of the T_g for thin films of homopolymers, it is concluded that also for homopolymer a highly mobile surface layer is relevant for the widely observed T_g depression.

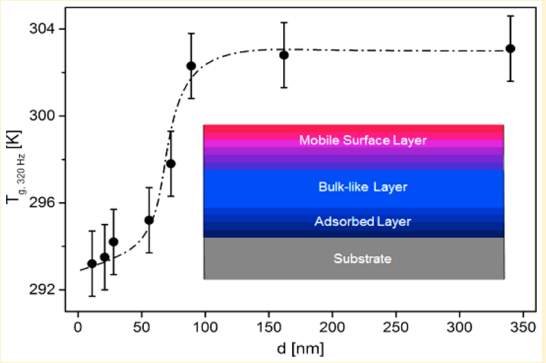

Downloaded by BUNDESANSTALT MATERIALFORSCHUNG on September 7, 2015 | http://pubs.acs.org
Publication Date (Web): July 15, 2015 | doi: 10.1021/acs.macromol.5b01259

1. INTRODUCTION

Although glasses have been used by mankind since ancient times, a strong interest in the understanding of their dynamical, rheological, and thermal properties is still there for several decades now.[1−3] The glass transition is one of the most important unsolved problems in condensed matter science and is related to many aspects of materials research. Besides bulk properties,[1] progress has been made to elucidate the glass transition in ultrathin polymer films (see, for instance, refs 4−12 and quoted references), which was discussed controversially. In thin films interfaces or boundary layers play a major role including the formation of dynamic heterogeneities. From the point of innovative technologies, the interest in ultrathin films is due to their wide applications in coatings, membranes, and organic electronic devices. For all these applications the glass transition temperature T_g is the key parameter. For example, polymeric layers with nanometer thicknesses used as resist materials require a given mechanical stability for processing.[13] Moreover, polymer-based nanocomposites are used to reinforce tires, where their properties are dominated by a thin polymer layer close to a nanoparticle.[15] Finally, the performance of sensors and/or batteries depends on the mobility of polymer segments in a layer adjacent to a solid surface.

From the scientific point of view, ultrathin polymer films provide ideal sample geometry to study confinement effects. Since the work of Keddie and Jones,[16,17] a variety of studies have been carried out on the thickness dependence of T_g, which are controversially discussed. For the same sample system (polymer and substrate) divergent results were obtained. Nevertheless, one has to differentiate between two kinds of experiments. First, in so-called static experiments, a thermodynamic property[16,17] (or an associated quantity) is measured during temperature ramping. A kink-like change in its temperature dependence is interpreted as thermal glass transition, and a thermal T_g can be extracted. Examples are ellipsometry,[16−19] fluorescence spectroscopy,[20] and dielectric expansion dilatometry.[22] Second, techniques that explore the segmental mobility directly like dielectric (see refs 11 and 21−24) and specific heat spectroscopy (see refs 11 and 25−27) are employed to investigate the dynamic glass transition of polymeric films. For these methods the data are taken at temperatures above the thermal T_g, which is an essential difference to the static experiments.

As a general result, it was found that in ultrathin polymeric films the thermal T_g can deviate substantially from the bulk value. The most surprising result is reported for polymers having a nonattractive interaction with the substrate.[17] Here, a depression of T_g with decreasing film thickness is observed (see refs 16−18 and 28−30). For free-standing films, this depression is found to be more pronounced[31] and depends strongly on molecular weight.[32]

Nowadays, the dependence of the thermal T_g on the thickness of a supported thin film is discussed by a counterbalance of a substrate and a surface effect (see Figure 1A).[5,18] On the one hand, the former effect is due to an interaction of the polymer segments with the substrate. For attractive interactions, this will lead to the formation of a boundary layer with a reduced segmental mobility and to an increase of the T_g. On the other hand, a T_g depression is discussed as the result of a free surface (polymer/air). Because of missing segment interactions and other structural differences,

Received: June 10, 2015
Revised: July 1, 2015
Published: July 15, 2015

 © 2015 American Chemical Society

DOI: 10.1021/acs.macromol.5b01259
Macromolecules 2015, 48, 4936−4941

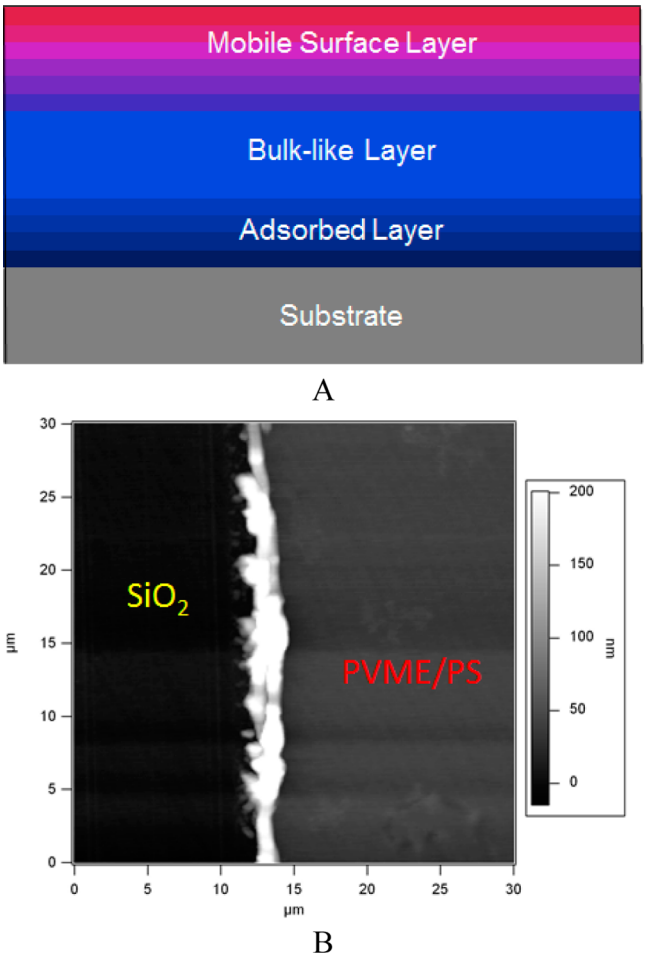

Figure 1. (A) Schematic of the structure of thin films. (B) AFM image of scratch of a PVME/PS blend film with a thickness of 39 nm after annealing. No sign of dewetting or phase separation is observed.

this surface layer should have a higher molecular mobility than the bulk and consequently a lower thermal T_g. Several experiments provide evidence for a mobile surface layer like photobleaching experiments[6] or embedding of gold nanospheres into a surface.[33,34]

In contrary to static experiments, results obtained by dynamic methods often show that the dynamic T_g is thickness independent,[11,25−27] causing a controversial discussion. The photobleaching experiments also deliver the thickness of the surface layer including its temperature dependence.[6] Above T_g, the thickness of the surface layer decreases with increasing temperature. Therefore, the influence of the surface layer on a measured dynamic T_g decreases with increasing temperature. This effect might be the reason why dynamic methods show no change of the dynamic T_g while the thermal T_g estimated in static experiments decreases with decreasing film thickness.[35,36]

Here, the glass transition behavior of ultrathin films of a polymer blend which is miscible in the bulk is investigated by specific heat spectroscopy using ac chip calorimetry.[25] As homopolymers polystyrene (PS) and poly(vinly methyl ether) (PVME) were used. For the bulk, the structure of a polymer blend is well understood, but for its molecular dynamics several open questions remain. Especially the composition dependence of the molecular dynamics is known to be complex.[37] The segmental dynamics is heterogeneous because the mixing of the components is not completely random. There is a higher probability that a given segment is surrounded by the same type of segments. Therefore, the local effective concentration is different from the average composition of the blend. This effect is due to chain connectivity and can be modeled by the self-concentration approach.[37] Also, temperature driven concentration fluctuations will take place.[37] For thin films of miscible polymers, an additional effect must be considered. In the absence of entropic effects, the composition at the free surface is dominated by the component, which has the lower cohesive energy.[38,39] For PVME/PS this was demonstrated for instance by X-ray photoelectron spectroscopy (XPS)[40] or spectroscopic ellipsometry.[41] The preferential surface segregation of the one component will lead to thickness-dependent phase transition and dewetting temperatures.[42−44]

From a general point of view the surface segregation can be considered as a self-assembling process, which leads to a structure with a nanometer thin layer on the polymer/air interface, having a higher molecular mobility. It was demonstrated that the chain dynamics, in the PVME enriched surface layer of a PMEV/PS blend system, was enhanced with regard to the bulk.[45] Here for the first time a highly mobile surface layer was evidenced by calorimetric experiments sensing the dynamic glass transition directly.

2. EXPERIMENTAL SECTION

Materials. The polymers were purchased from Aldrich Inc. PS has a molecular weight (M_w) of 524 kg/mol and a polydispersity index (PI) of 1.04. The T_g of PS is 103 °C. PVME was obtained as an aqueous solution (50 wt %) and has a M_w of 60 kg/mol, a PI of 3, and a T_g of −26 °C. PVME was dried under vacuum at 40 °C for 72 h. PVME/PS blend of 50/50 weight ratio was dissolved in toluene.

Film Preparation. The films were prepared on the surface of the sensor (XEN 39390, Xensor integrations, Nl), used for the measurements by differential ac chip calorimetry. The sensor was cleaned by dropping a drop of toluene to its center followed by spinning. This procedure was repeated three times, followed by annealing under vacuum at 473 K for 2 h to cure the epoxy resin, which was used to glue the chip to the housing.

Thin films were obtained by spin-coating a filtered (Minipore, 0.2 μm) solution of PVME/PS in toluene (3000 rpm, 30 s) onto the central part of the sensor. The film thickness was adjusted by the concentration of the solution. After spin-coating, all samples were dried in an oil-free vacuum (10^{-4} mbar) for 24 h at room temperature and further annealed at 50 °C ($T_{ann} = T_{g,bulk} + 45$ K) for 72 h in order to remove the solvent and the stress induced by the spin-coating procedure.[46]

Because the thickness d of the thin films cannot be measured on the sensor, a second set of films were prepared under identical conditions on a silicon wafer to estimate d by atomic force microscopy (AFM). Since the silicon wafer has similar surface properties than the sensor, it is assumed that under identical spin-coating conditions the film on silicon wafer has the same thickness as that supported by the sensor.

AFM images of the films before and after the annealing procedure further show homogeneous films with a low roughness even for the thinnest films. No sign of dewetting was observed. As an example, Figure 1b gives the AFM image of a scratch across a PVME/PS film with a thickness of ca. 39 nm on a silicon wafer.

Differential AC Chip Calorimetry. At the calorimeter chip the heater is located in the center of a free-standing thin silicon nitride membrane (thickness 1 μm) supported by a Si frame. The chip has a theoretical heated hot spot area of about 30 × 30 μm^2, with an integrated 6-couple thermopile and two 4-wire heaters.[47] In addition to the hot spot, the heater strips contribute to the heated area as well. A SiO_2 layer (thickness 0.5−1 μm) protects the heater and thermopile. The thin film was spin coated over the whole sensor, but only the small heated area is sensed and can be considered as a point heat source.

Downloaded by BUNDESANSTALT MATERIALFORSCHUNG on September 7, 2015 | http://pubs.acs.org
Publication Date (Web): July 15, 2015 | doi: 10.1021/acs.macromol.5b01259

DOI: 10.1021/acs.macromol.5b01259
Macromolecules 2015, 48, 4936−4941

The differential approach minimizes the contribution of the heat capacity of the empty sensor to the measured data.[25] In the approximation of thin films (submicron) the heat capacity of the sample C_s is then given by

$$C_s = i\omega C_{eff}(\Delta U - \Delta U_0)/P_0 S \quad (1)$$

Here ω is the radial frequency, $\omega = 2\pi f$, where f is frequency, S sensitivity of the thermopile, and P_0 applied heating power. $C_{eff} \equiv C_0 + G/i\omega$ describes the effective heat capacity of the empty sensor where $G/i\omega$ is the heat loss through the surrounding atmosphere. ΔU is the complex differential thermopile signal for an empty and a sensor with a sample, and ΔU_0 is the complex differential voltage measured for two empty sensors. Absolute values of C_s can be deduced using calibration techniques. Here the real part of the complex differential voltage and the phase angle are considered.

During the measurement the frequency was kept constant while the temperature was scanned with a rate of 1−2.0 K/min depending on the frequency. The heating power for the modulation was kept constant at about 25 μW, which ensures that the amplitude of the temperature modulation is less than 0.25 K. The frequency is varied between 1 and 10^4 Hz.

X-ray Photoelectron Spectroscopy (XPS). For the XPS measurements a SAGE 150 (Specs, Berlin, Germany) spectrometer equipped with a hemispherical analyzer (Phoibos 100 MCD-5) is used. Nonmonochromatic Mg Kα radiation (11 kV, 220 W) was employed at a pressure of ca. 10^{-7} Pa in the analysis chamber. The angle between the axis of X-ray source and the analyzer lenses was 54.9°. The analyzer was mounted at 18° to the surface normal. XPS spectra were acquired in the constant analyzer energy mode. The information depth of XPS measurements is between 3 and 7 nm.

Differential Scanning Calorimetry (DSC). DSC has been carried out for the bulk samples employing a differential scanning calorimeter (DSC 220C, rates 10 K/min). N_2 is used as protection gas.

3. RESULTS AND DISCUSSION

Figure 2 depicts the result of an ac calorimetry measurement at a frequency of 160 Hz for a polystyrene film with a thickness of 59 nm. The measurement gives a complex differential voltage, which is proportional to the complex heat capacity of the film (C_s; see eq 1) as a function of temperature at the selected frequency. The real part of the complex differential voltage U_R and the phase angle ϕ are taken as measures of C_s here. At the dynamic glass transition, U_R increases stepwise with increasing temperature (Figure 2A) where ϕ shows a peak (Figure 2B). In the raw data of ϕ (Figure 2B), there is an underlying step in the signal, which is proportional to the step in U_R. Therefore, the phase angle is corrected by subtracting this contribution (Figure 2B). A dynamic T_g can be determined as the half step temperature of U_R or as the maximum temperature of the peak of the corrected phase angle.

Figure 3A gives the DSC curves for PVME, PS, and PVME/PS (50/50 wt %). Data for the blend shows the broadening of the glass transition zone, as known from the literature,[37] which can be understood within the self-concentration as well as in the temperature driven concentration fluctuation approach.[37]

This broadening of the glass transition is also confirmed by the ac chip calorimetry on thin films (see Figure 3B). For the blend film both U_R and ϕ show considerable broadening of its widths compared to the homopolymers.

The ac chip calorimetry investigation for ultrathin PS[25,35] and PVME[27] films shows that the dynamic T_g is independent of the film thickness down to several nanometers (see also Figure 4B and inset in Figure 5A). Figure 4A depicts ϕ for thin blend films versus temperature for different thicknesses. In contrast to the homopolymers, for the blends the dynamic T_g decreases systematically with decreasing film thickness. This shift of T_g is

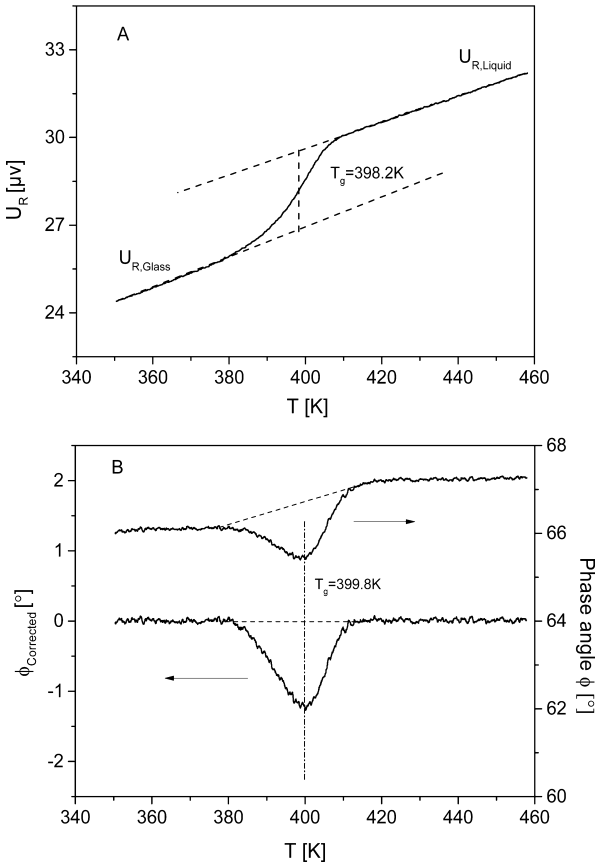

Figure 2. Real part (A) and phase angle (B) of the complex differential voltage of a PS film (59 nm, f = 160 Hz). The contribution of the underlying step in the heat capacity in the raw data of ϕ (upper panel) was subtracted from the curve (lower panel).

much larger than the error of an ac chip calorimetry measurement, which is 2−3 K.

From the peak position of the phase angle, the dynamic T_g is estimated for the given frequency, and the relaxation map can be constructed (Figure 4B). For the dynamic glass transition, the temperature dependence of the relaxation rate f_p is curved when plotted versus $1/T$, which can be described by the Vogel−Fulcher−Tammann (VFT) equation.[48] As discussed above, for pure PVME the data for all film thicknesses collapse into one chart (see also ref 27). The same behavior was observed for polystyrene (see inset of Figure 4B).[35] However, for the blends the whole trace of the dynamic glass transition shifts to lower temperatures with decreasing film thickness.

To discuss this thickness dependence in detail the dynamic T_g measured at 320 Hz is plotted versus film thickness (Figure 5A). As already stated, for both homopolymers the dynamic T_g is independent of d (inset of Figure 5A). For the blends for d > 100 nm the T_g is independent of thickness. At around 80 nm T_g starts to decrease with decreasing film thickness by around 12 K.

The following model is assumed to discuss the thickness dependence of the dynamic T_g of thin polymer blend films (Figure 1A). In the middle of the film, a more or less bulk-like behavior is preserved. As discussed above, PVME has a lower surface tension, with respect to air, than polystyrene. This means a PVME-rich surface layer is formed at the air/polymer interface by self-assembling. Because of the higher PVME concentration, it should have a higher molecular mobility than a

Downloaded by BUNDESANSTALT MATERIALFORSCHUNG on September 7, 2015 | http://pubs.acs.org
Publication Date (Web): July 15, 2015 | doi: 10.1021/acs.macromol.5b01259

DOI: 10.1021/acs.macromol.5b01259
Macromolecules 2015, 48, 4936−4941

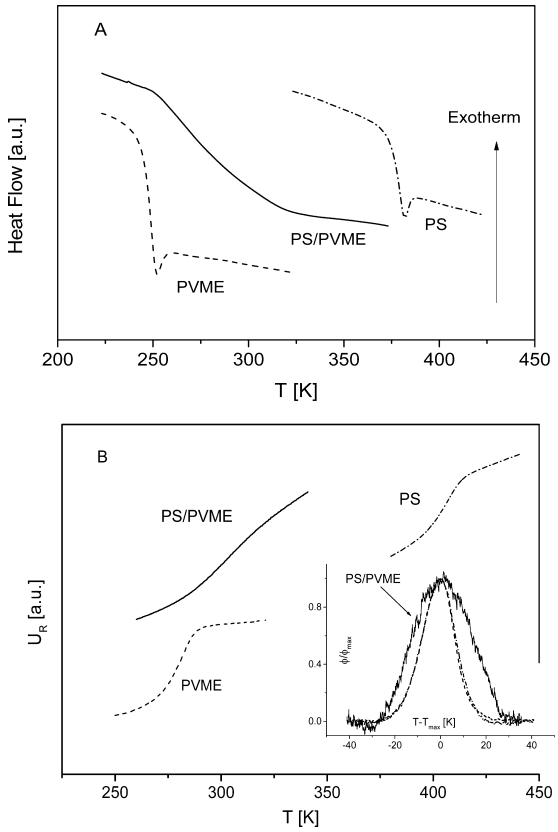

Figure 3. (A) DSC trace (second heating run; rate: 10 K/min) for PVME (dashed), PS (dashed dotted), and PVME/PS blend (50/50 wt %, solid). (B) Real part of the complex differential voltage U_R versus temperature for films: dashed line = PVME, thickness 192 nm; dashed dotted line = PS, thickness 280 nm; solid line = PVME/PS (50/50 wt %), thickness 162 nm. The frequency of the measurement was 480 Hz and the rate 2 K/min. The inset gives the corresponding phase angles normalized with respect to its maximum value and the peak temperature.

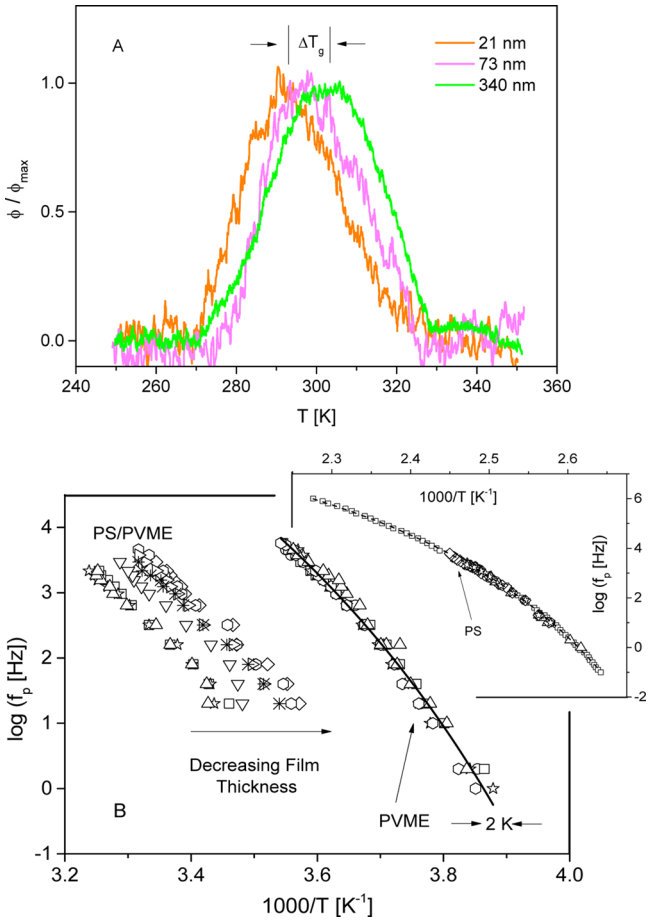

Figure 4. (A) Normalized phase angle of the complex differential voltage measured by specific heat spectroscopy for thin films of the polymer blend PVME/PS (50/50 wt %) at a frequency of 320 Hz for the indicated film thicknesses. (B) Relaxation map for PVME and for PVME/PS films (50/50 wt %) for different film thicknesses. PVME: triangles, 12 nm; hexagons, 58 nm; stars, 168 nm; squares, 192 nm; circles, 218 nm. The solid line is a fit of the VFT equation to all data of PVME. PVME/PS blend: diamonds, 11 nm; hexagons, 21 nm; right-pointing triangles, 28 nm; asterisks, 56 nm; down-pointing triangles, 73 nm; squares, 89 nm; stars, 162 nm; up-pointing triangles, 340 nm. The inset gives the relaxation map for pure PS films: stars, 18 nm; diamonds, 52 nm; triangles, 280 nm; circles, 3000 nm; squares, dielectric data for bulk PS. The line is VFT fit using all data. The data for the inset are taken from ref 35.

50/50 wt % film and hence a lower dynamic T_g. Ac chip calorimetry measures the thermal response across the whole film thickness. With decreasing film thickness, the relative influence of the PVME-rich surface layer on the thermal response of the film increases. Therefore, T_g of the whole film decreases.

To evidence the PVME-rich layer directly, XPS measurements were employed to estimate the concentration of PVME in a surface layer with a thickness of 3−5 nm, as PVME contains oxygen in contrast to polystyrene. The inset of Figure 5B shows the C1 XPS spectrum of a PVME/PS blend film (50/50 wt %, thickness of 200 nm). The C−H and C−O bonds can be observed as separated peaks.[49] Two Gaussians are fitted to the data to estimate the areas of both peaks (I_{C-O} and I_{C-H}). For the weight fraction w of PVME, one obtains[43]

$$\frac{I_{C-O}}{I_{C-H}} = \frac{2w/M_{VME}}{\frac{8(1-w)}{M_S} + \frac{3w}{M_{VME}}} \quad (2)$$

where M_{VME} and M_S are the molecular weights of the repeating units of PVME and PS, respectively. The concentration of PVME was calculated to 83 wt % at the air/polymer interface, and the PVME-rich surface layer is confirmed. Since the observed thickness dependence of the dynamic T_g is similar to the thickness dependence of the thermal T_g for thin films of homopolymers, it is concluded that also for homopolymer systems a highly mobile surface layer is relevant for thermal T_g depression.

The Fox equation[50]

$$\frac{1}{T_{g,blend}} = \frac{1-w}{T_{g,PS}} + \frac{w}{T_{g,PVME}} \quad (3)$$

describes the composition dependence of T_g of miscible polymer blends. By reformulating eq 3, the composition can be calculated in dependence on d if the T_gs are known (Figure 5B). For large film thicknesses, the concentration of PVME of the film is independent of d. With decreasing film thickness w increases and reaches the value estimated by XPS.

Surprisingly, the PVME concentration estimated by the Fox equation for thick bulk-like films is not 50 wt % as formulated but ca. 71 wt %. For a different polymer system (75 wt % PS/25 wt % PVME) the thickness of the segregated surface layer

Downloaded by BUNDESANSTALT MATERIALFORSCHUNG on September 7, 2015 | http://pubs.acs.org
Publication Date (Web): July 15, 2015 | doi: 10.1021/acs.macromol.5b01259

DOI: 10.1021/acs.macromol.5b01259
Macromolecules 2015, 48, 4936−4941

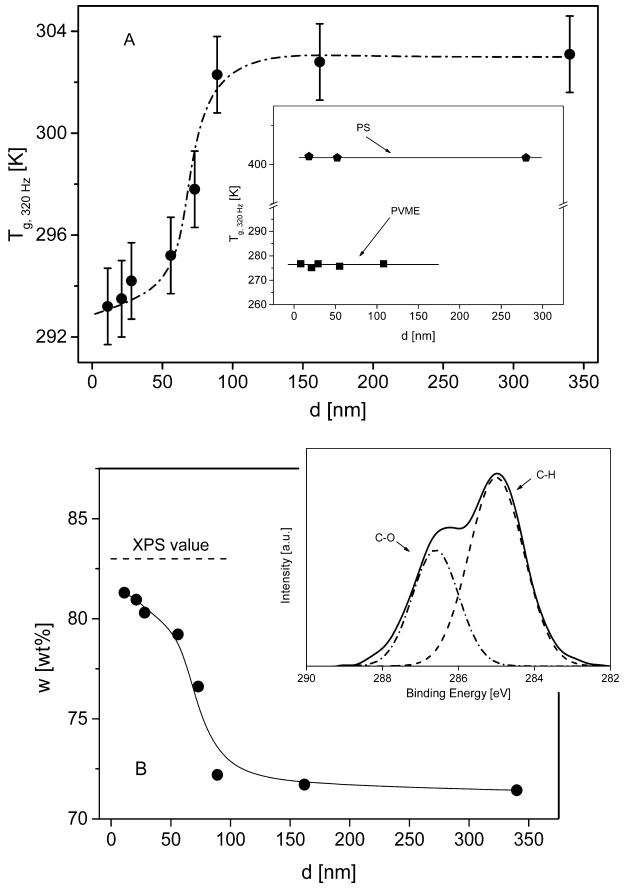

Figure 5. (A) Dynamic glass transition temperature measured at 320 Hz versus film thickness d for PVME/PS blend films (50/50 wt %). The line is a guide for the eyes. The inset gives T_g measured at 320 Hz versus film thickness d for the PS and PVME. The lines represent the average values. (B) Concentration of PVME versus d as estimated from the Fox equation. The line is a guide to the eyes. The inset gives the C1 XPS spectrum of a PVME/S (50/50 wt %, d = 200 nm). The dashed lines represent the fitted Gaussians.

was found to be between 5 and 10 nm for the considered thickness range.[45] Therefore, for thick films of several 100 nm, the bulk-like layer in the middle of the layer should dominate the calorimetric response. From the extracted higher value of the PVME concentration of 71 wt % found for thick blend films, one has to conclude that there is a polystyrene-rich layer adsorbed at the substrate to minimize the interaction energy of the polymer system with the SiO_2 surface. This is in agreement with results found by SIMS investigations on a deuterated PVME/dPS system.[43]

4. CONCLUSION

In conclusion, this is the first report of the thickness dependence of T_g of ultrathin films of a polymer blend, which is miscible in the bulk. This shift is due to the self-assembling of a nanometer thick surface layer with a higher molecular mobility, formed at the top. Starting at ca. 100 nm, T_g decreases with decreasing film thickness. Since the observed behavior of T_g is similar to that of ultrathin films of homopolymers, it is concluded that a nanometer thick surface layer is also relevant in the latter case.

AUTHOR INFORMATION

Corresponding Author

*Tel +49 30/8104-3384; Fax +49 30/8104-1617; e-mail Andreas.Schoenhals@bam.de (A.S.).

Notes

The authors declare no competing financial interest.

ACKNOWLEDGMENTS

The authors thank the German Science Foundation DFG for financial support (SCHO 440/20-1; SCHO 440/20-2).

REFERENCES

(1) Ediger, M.; Harrowell, P. *J. Chem. Phys.* **2012**, *137*, 080901.
(2) Debenedetti, P. G.; Stillinger, F. H. *Nature* **2001**, *410*, 259−267.
(3) Anderson, P. W. *Science* **1995**, *267*, 1615.
(4) O'Connell, P. A.; McKenna, G. B. *Science* **2005**, *307*, 1760−1763.
(5) Ediger, M.; Forrest, J. A. *Macromolecules* **2014**, *47*, 471−478.
(6) Paeng, K.; Swallen, S. F.; Ediger, M. D. *J. Am. Chem. Soc.* **2011**, *133*, 8444−8447.
(7) Forrest, J. A.; Dalnoki-Veress, K. *Adv. Colloid Interface Sci.* **2001**, *94*, 167−196.
(8) Forrest, J. A. *Eur. Phys. J. E* **2002**, *8*, 261−266.
(9) Fakhraai, Z.; Forrest, J. A. *Science* **2008**, *319*, 600−604.
(10) Chai, Y.; Salez, T.; McGraw, J. D.; Benzaquen, M.; Dalnoki-Veress, K.; Raphaël, E.; Forrest, J. A. *Science* **2014**, *343*, 994.
(11) Tress, M.; Erber, M.; Mapesa, E. U.; Huth, H.; Müller, J.; Serghei, A.; Schick, C.; Eichhorn, K.-J.; Voit, B.; Kremer, F. *Macromolecules* **2010**, *43*, 9937−9944.
(12) Tress, M.; Mapesa, E. U.; Kossack, W.; Kipnusu, W. K.; Reiche, M.; Kremer, F. *Science* **2013**, *341*, 1371−1374.
(13) Delcambre, S. P.; Riggleman, R. A.; de Pablo, J. J.; Nealey, P. F. *Soft Matter* **2010**, *6*, 2475−2483.
(14) Papon, A.; Montes, H.; Hanafi, M.; Lequeux, F.; Guy, L.; Saalwächter, K. *Phys. Rev. Lett.* **2012**, *108*, 065702.
(15) Füllbrandt, M.; Purohit, P. J.; Schönhals, A. *Macromolecules* **2013**, *46*, 4626−4632.
(16) Keddie, J. L.; Jones, RA.; Cory, R. A. *Faraday Discuss.* **1994**, *98*, 219−230.
(17) Keddie, J. L.; Jones, R. A.; Cory, R. A. *Euro Phys. Lett.* **1994**, *27*, 59−64.
(18) Forrest, J.; Dalnoki-Veress, K. *Adv. Colloid Interface Sci.* **2001**, *94*, 167−196.
(19) Efremov, M. Y.; Kiyanova, A. V.; Last, J.; Soofi, S. S.; Thode, C.; Nealey, P. F. *Phys. Rev. E* **2012**, *86*, 021501.
(20) Ellison, C. J.; Torkelson, J. M. *Nat. Mater.* **2003**, *2*, 695−700.
(21) Napolitano, S.; Pilleri, A.; Rolla, P.; Wübbenhorst, M. *ACS Nano* **2010**, *4*, 841−848.
(22) Yin, H.; Napolitano, S.; Schönhals, A. *Macromolecules* **2012**, *45*, 1652−1662.
(23) Napolitano, S.; Wübbenhorst, M. *Nat. Commun.* **2011**, *2*, 260.
(24) Labahn, D.; Mix, R.; Schönhals, A. *Phys. Rev. E* **2009**, *79*, 011801.
(25) Huth, H.; Minakov, A.; Schick, C. Differential. *J. Polym. Sci., Part B: Polym. Phys.* **2006**, *44*, 2996−3005.
(26) Yin, H.; Schönhals, A. *Soft Matter* **2012**, *8*, 9132−9139.
(27) Yin, H.; Schönhals, A. *Polymer* **2013**, *54*, 2067−2070.
(28) Lupaşcu, V.; Picken, S. J.; Wübbenhorst. *J. Non-Cryst. Solids* **2006**, *352*, 5594−5600.
(29) Fakhraai, Z.; Forrest, J. *Phys. Rev. Lett.* **2005**, *95*, 025701.
(30) Sharp, J. S.; Forrest, J. A. *Phys. Rev. Lett.* **2003**, *91*, 235701.
(31) Forrest, J.; Dalnoki-Veress, K.; Dutcher, J. *Phys. Rev. E: Stat. Phys., Plasmas, Fluids, Relat. Interdiscip. Top.* **1997**, *56*, 5705−5716.
(32) Dalnoki-Veress, K.; Forrest, J.; Murray, C.; Gigault, C.; Dutcher, J. R. *Phys. Rev. E: Stat. Phys., Plasmas, Fluids, Relat. Interdiscip. Top.* **2001**, *63*, 031801.
(33) Qi, D.; Ilton, M.; Forrest, J. *Eur. Phys. J. E: Soft Matter Biol. Phys.* **2011**, *34*, 56.

Downloaded by BUNDESANSTALT MATERIALFORSCHUNG on September 7, 2015 | http://pubs.acs.org
Publication Date (Web): July 15, 2015 | doi: 10.1021/acs.macromol.5b01259

DOI: 10.1021/acs.macromol.5b01259
Macromolecules 2015, 48, 4936−4941

(34) Qi, D.; Daley, C. R.; Chai, Y.; Forrest, J. *Soft Matter* **2013**, *9*, 8958−8964.
(35) Boucher, V. M.; Cangialosi, D.; Yin, H.; Schönhals, A.; Alegria, A.; Colmenero. *Soft Matter* **2012**, *8*, 5119−5122.
(36) Yin, H.; Cangialosi, D.; Schönhals, A. *Thermochim. Acta* **2013**, *566*, 186−192.
(37) Colmenero, J.; Arbe, A. *Soft Matter* **2007**, *3*, 1474−1485.
(38) Nakanishi, H.; Pincus, P. *J. Chem. Phys.* **1983**, *79*, 997−1003.
(39) Schmidt, I.; Binder, K. *J. Phys. (Paris)* **1985**, *46*, 1631−1644.
(40) Bhatia, Q. S.; Pan, D. H.; Koberstein, J. T. *Macromolecules* **1988**, *21*, 2166−2175.
(41) Thomas, K. R.; Clarke, N.; Poetes, R.; Morariu, M.; Steiner, U. *Soft Matter* **2010**, *6*, 3517−3523.
(42) Gotzen, N.; Huth, H.; Schick, C.; Assche, G.; Neus, C.; Mele, B. *Polymer* **2010**, *51*, 647−654.
(43) Tanaka, K.; Yoon, J.-S.; Takahara, A.; Kajiyama, T. *Macromolecules* **1995**, *28*, 934−938.
(44) Xia, T.; Ogawa, H.; Inoue, R.; Yamada, N. L.; Li, G.; Kanaya, T. *Macromolecules* **2013**, *46*, 4540−4547.
(45) Frieberg, B.; Kim, J.; Narayanan, S.; Green, P. F. *ACS Macro Lett.* **2013**, *2*, 388−392.
(46) Reiter, G.; Hamieh, M.; Damman, P.; Sclavons, S.; Gabriele, S.; Vilmin, T.; Raphael, E. *Nat. Mater.* **2005**, *4*, 754−758.
(47) van Herwaaden, S. Application note for Xsensor's calorimtere chips of XEN-39390 series http://www.xensor.nl/pdffiles/sheets/nanogas3939.
(48) Vogel, H. *Phys. Z.* **1921**, *22*, 645. Fulcher, G. S. *J. Am. Chem. Soc.* **1925**, *8*, 339−355. Tammann, G.; Hesse, W. *Z. Anorg. Allg. Chem.* **1926**, *156*, 245.
(49) Beamson, G.; Briggs, H. *High Resolution XPS of Organic Polymers: The Scienta ESCA 300 Database*; Wiley: Chichester, UK, 1992.
(50) Hiemenz, P.; Lodge, T. *Polymer Chemistry*, 2nd ed.; CRC Press: Boca Raton, FL, 2007.

Downloaded by BUNDESANSTALT MATERIALFORSCHUNG on September 7, 2015 | http://pubs.acs.org
Publication Date (Web): July 15, 2015 | doi: 10.1021/acs.macromol.5b01259

DOI: 10.1021/acs.macromol.5b01259
Macromolecules 2015, 48, 4936−4941